Journal of
Composites Science

MDPI

Article

Processing and Evaluation of an Aluminum Matrix Composite Material

Calin-Octavian Miclosina [1], Remus Belu-Nica [2], Costel Relu Ciubotariu [1,*] and Gabriela Marginean [3]

[1] Department of Engineering Science, Faculty of Engineering, Babeș-Bolyai University, Traian Vuia Square 1–4, 320085 Resita, Romania; calin.miclosina@ubbcluj.ro
[2] Bona Dea Imex, Str. Valiugului, no. 60 C, 320011 Resita, Romania; remusbelu.nica@gmail.com
[3] Institute of Mechanical Engineering, Westphalian University of Applied Sciences Gelsenkirchen Bocholt Recklinghausen, Neidenburger Str. 43, 45897 Gelsenkirchen, Germany; gabriela.marginean@w-hs.de
* Correspondence: relu.ciubotariu@ubbcluj.ro

Abstract

This study signifies the development and characterization of a composite material with a metallic matrix of aluminum reinforced with a steel mesh, utilizing centrifugal casting technology. An evaluation was conducted to ascertain the influence of the formulation process and the presence of the insert on the mechanical behavior with regard to tensile strength. The aluminum matrix was obtained from commercial and scrap alloys, elaborated by advanced methods of degassing and chemical modification. Meanwhile, the steel mesh reinforcement was cleaned, copper plated, and preheated to optimize wetting and, consequently, adhesion. The structural characterization was performed by scanning electron microscopy (SEM) and energy dispersive X-ray spectroscopy analyses (EDX), which highlighted a well-defined interface and uniform copper distribution. The composite was produced by means of horizontal-axis centrifugal casting in a fiberglass mold, followed by cold rolling to obtain flat specimens. A total of eight tensile specimens were examined, with measured ultimate tensile strengths ranging from 78.5 to 119.8 (MPa). A thorough examination of the fractured specimens revealed a brittle fracture mechanism, devoid of substantial plastic deformation. The onset of failures was frequently observed at the interface between the aluminum matrix and the steel mesh. The use of SEM and EDX investigations led to the confirmation of the uniformity of the copper coating and the absence of significant porosity or interfacial defects. A bimodal distribution of tensile strength values was observed, a phenomenon that is likely attributable to variations in mesh positioning and local differences in solidification. A correlation was established between the experimental results and an analytical polynomial model, thereby confirming a reasonable fit. In sum, the present study provides a substantial foundation for the development of metal matrix composites with enhanced performance, specifically designed for challenging structural applications. This method also demonstrates potential for recycling aluminum scrap into high-performance composites with controlled microstructure and mechanical integrity.

Keywords: composite material; aluminum matrix; steel mesh; centrifugal casting; tensile testing; microstructural characterization

check for updates

Academic Editor: Prashanth Konda Gokuldoss

Received: 15 May 2025
Revised: 14 June 2025
Accepted: 25 June 2025
Published: 27 June 2025

Citation: Miclosina, C.-O.; Belu-Nica, R.; Ciubotariu, C.R.; Marginean, G. Processing and Evaluation of an Aluminum Matrix Composite Material. *J. Compos. Sci.* **2025**, *9*, 335. https://doi.org/10.3390/jcs9070335

Copyright: © 2025 by the authors. Licensee MDPI, Basel, Switzerland. This article is an open access article distributed under the terms and conditions of the Creative Commons Attribution (CC BY) license (https://creativecommons.org/licenses/by/4.0/).

1. Introduction

Aluminum metal matrix composites (AMMCs) represent a promising category of advanced materials for modern industry needs. These composites are used in numerous applications due to their unique combination of mechanical, physical, and tribological

properties. These materials are distinguished by their low weight, high resistance to wear and corrosion, and exceptional mechanical performance, which renders them indispensable in various fields [1–3]. AMMCs have found extensive application in the automotive industry, particularly in the production of critical components such as brake rotors, pistons, and engine blocks. In these applications, it is essential to balance several factors, including weight, mechanical performance, and cost [4–6]. In the aerospace industry, these materials are preferred due to their ability to withstand extreme temperatures and wear conditions while maintaining a low weight [4,6]. In the robotics industry, the utilization of these materials is recommended for the fabrication of structural components, transmission elements, and precision parts. This ensures the maintenance of rigidity, dimensional stability, and resistance to various types of wear [7–9].

Recent studies emphasize that metal matrix nanocomposites (MMNCs), a subclass of AMMCs, offer significant performance improvements when reinforced with particles such as SiC, Al_2O_3, TiO_2, graphene, or even biogenic sources like palm sprout shell ash. These materials have demonstrated notable gains in hardness (up to +13.9%), tensile strength (+24.0%), and compression strength (+32.9%) with only 6 wt.% reinforcement content [10]. This has enabled their integration into components with critical mechanical demands, such as engine elements, heat exchangers, aerospace coatings, and precision mechanical structures. Moreover, the use of MMNCs is growing in the fields of advanced electronics, data storage systems, and micro-devices (MEMS). In these areas, the properties of thermal conductivity, dimensional stability, and reduced weight are of paramount importance. Despite the higher costs associated with these materials, their ability to tailor their properties to specific functional needs renders them highly competitive and innovative for next-generation applications [11–14].

The primary objective of the development of these materials is to enhance the performance of components under challenging operating conditions, while concurrently reducing energy consumption and carbon emissions [15,16]. The enhanced mechanical properties of AMMC are attributable to the incorporation of reinforcing particles, including carbides, oxides, nitrides, and both continuous and discontinuous fibers. These particles are critical for enhancing tensile strength, durability, and fatigue behavior [17,18]. For instance, the utilization of glass or carbon fibers, in conjunction with aluminum alloys, yields materials that exhibit an optimal strength-to-weight ratio, rendering them particularly well-suited for structural applications [19–21]. Moreover, recent research has underscored the efficacy of hybrid materials, which integrate diverse reinforcing particles to optimize costs and performance [22,23].

Beyond the reinforcement particle design, the processing route exerts a substantial influence on the final material properties. Concurrent with these contemporary advancements, additive manufacturing (AM) technologies, such as selective laser melting (SLM), have garnered mounting interest in the fabrication of AMMC with sophisticated microstructures and augmented mechanical performance, particularly for applications in the aerospace and biomedical domains. Ponnusamy et al. conducted a review that provides a comprehensive overview of the mechanical response of SLM-processed aluminum alloys [24]. The review emphasizes the critical influence of process parameters on density, porosity, and strength. These process parameters include build orientation, scan strategy, and post-processing.

Conventional approaches, such as centrifugal casting, persist as viable and cost-effective alternatives, particularly when recycled aluminum alloys are utilized. The present study proposes an accessible manufacturing route that does not rely on metallic powders or the costly infrastructure typically associated with AM technologies. Instead, it achieves relevant mechanical performance by focusing on interface optimization between the metallic

matrix and a copper-coated steel mesh reinforcement. Consequently, this work contributes to the diversification of technological pathways for producing AMMC and highlights the potential of combining classical metallurgical methods with modern surface engineering strategies. In this context, the fabrication of AMMC presents a series of technical challenges. The uniform distribution and inadequate wetting of reinforcement particles in the metal matrix can result in agglomeration, thereby affecting the final mechanical properties [6,25–27]. The formation of pores during the manufacturing process has been demonstrated to have a substantial impact on the mechanical strength and durability of the composite [6,27,28].

Undesirable chemical reactions at the interface between the matrix and the particles have the potential to compromise the structural integrity of the material [6,29,30]. To address these limitations, advanced manufacturing technologies have been developed, including stir casting [31,32], infiltration by pressing [33], rotating active element friction processing [34,35], and centrifugal casting. These methods facilitate the attainment of uniform microstructures and enhance the mechanical and tribological properties of the materials. In light of the aforementioned considerations, the present research endeavor seeks to delineate the process of incorporating steel mesh through the utilization of centrifugal casting technology.

While the present study does not involve nanoscale reinforcements directly, it addresses a comparable challenge regarding enhancing the interface quality in metal matrix systems. The concept of copper-plated steel mesh utilized in this study aligns with the objectives of nanocomposite strategies, including enhanced bonding, reduced stress concentration, and increased mechanical reliability. This situates the research within the broader evolution of both micro- and nano-reinforced aluminum composites [10–14].

The originality of this work lies in its combination of centrifugal casting with a continuous steel mesh insert treated by galvanic copper plating, an approach that has rarely been explored in the extant literature. The present study proposes a methodology that integrates practical metallurgical engineering with mechanical analysis. This methodology is characterized by a focus on three key aspects: insert surface preparation, interfacial control, and the transformation of cast cylinders into testable flat samples through rolling. The integration of SEM/EDX data and analytical modeling provides a comprehensive evaluation of behavior at micro and macro scales. The integration of these elements, in conjunction with the utilization of contemporary literature, positions the present research as both methodologically rigorous and industrially relevant.

The primary objective of this study is to develop and validate a powder-free fabrication method for aluminum matrix composites. This method will be achieved by using centrifugal casting combined with a copper-coated steel mesh reinforcement. This approach is designed to enhance interfacial bonding, structural reliability, and mechanical performance, while circumventing the complexity and cost associated with alternative manufacturing technologies.

2. Materials and Methods

2.1. Materials

The raw material used to obtain the melt of the matrix consists of molten waste from aluminum-silicon alloys cast according to SR EN 1676:2020 [36] (to obtain max. 40% of the quantity) and pre-alloys with Al-Mg (10% Mg) and Al-Ti (6% Ti). The fondant's composition, determined by its weight, included Al-Si 2.5% and Hr (2%) as its primary constituents. The coating, refining, and modification process involved the use of a mixture of salts, including 62.5% NaCl, 25% NaF, and 12.5% KCl.

In order to achieve a controlled structure during the process of degassing, the utilization of liquid technical nitrogen at a concentration ranging from 0.2% to 0.4% was employed.

The melting process was carried out in a low-frequency electric furnace (IH-110, Across International, Bayswater, Australia) with an acid lining that was heated to a temperature range of 400 to 450 °C. The lining was thoroughly cleaned to ensure the absence of any slag or alloy residues from previous castings, ensuring the purity of the melting process. The materials matrix, which was to be subjected to melting, was characterized by its cleanliness, with the absence of oxides, moisture, oils, and calcination.

Concurrent with the evolution of the matrix material, the insert was formulated as a continuous steel wire mesh (OL37) with a diameter of 0.2 mm and square meshes with a side of 0.5 mm.

The matrix material was cast by means of the horizontal spindle casting facility (type UM-150-3518-00, designed and executed at the Machine Building Plant, Resita, Romania) into a fiberglass mold. In the process of steel mesh insert casting, the liquid alloy was subject to two forces: the force of gravity ($G = m \cdot g$) and the inertial force ($Fc = m \cdot \omega^2 \cdot r$), where m is the mass of the liquid alloy cast, ω is the angular velocity of the metal form, and r is the distance from the axis of rotation. These forces were uniformly distributed in the liquid mass. As illustrated in Figure 1, the casting and extraction of the cast piece are depicted schematically.

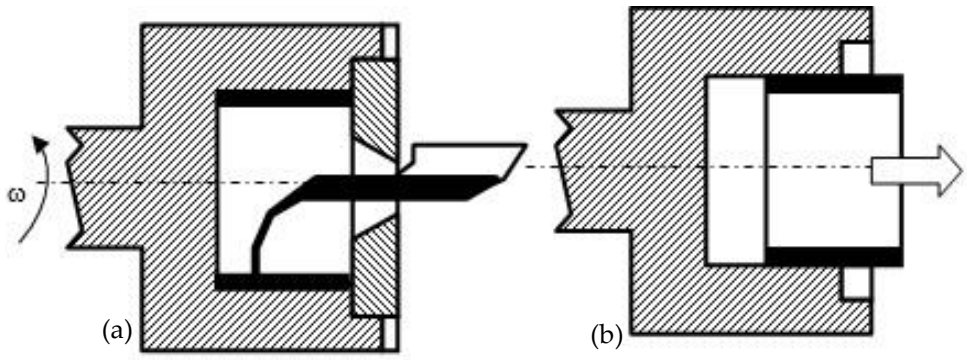


Figure 1. Centrifugal casting with horizontal axis of rotation: (**a**) pouring the liquid alloy into the metal form; (**b**) extracting the cast part from the mold [37].

In order to prevent deformations, the insert was clamped in the parting plane of the casting mold. The cylindrical prototypes obtained, reinforced with woven steel fibers in the form of a net, had a length of 240 mm and an outer diameter of 120 mm.

All chemical compositions presented in this study, including those in Tables 1 and 2, are expressed in weight percent (wt.%). The steel mesh insert was not quantified as a global mass or volume fraction of the composite; rather, it was introduced as a fixed-size structural element within the mold geometry. Therefore, the contribution was analyzed in terms of position, interface quality, and mechanical influence.

Table 1. Aluminum matrix chemical composition (wt.%).

Al	Si	Mn	Mg	Fe	Ti	Zn	Cu
87–89%	9–10%	0.3–0.6%	0.2–0.5%	0.6%	0.15%	0.10%	0.05%

Table 2. Steel fiber chemical composition (wt.%).

Fe	C	Mn	Si	P	S
98.70–99.40%	0.13–0.22%	0.3–0.6%	0.15–0.35%	0.045%	0.055%

2.2. Melting of the Matrix Alloy

Subsequent to the melting of the alloy (65%), the rapid heating process continued beneath a layer of fondant (flux) until the molten metal bath attained a temperature ranging from 700 to 730 °C. At this temperature, the objective of pre-degassing is to induce a thermal shock by rapidly introducing the entirety of the solid material into the metal bath. This results in a precipitous decline in the liquid bath's temperature, reaching levels between 580 and 600 °C. Subsequently, the molten bath was heated to 650 °C, and the slag was removed from the surface of the metal bath. In the subsequent stage of the process, the melting bath was covered with approximately 25% of the fondant.

Thereafter, the molten alloy underwent a double degassing operation, which involved the bubbling of nitrogen and the addition of almed tablets. The degassing process with nitrogen entailed the bubbling of the bath with a gentle current of nitrogen for a duration of 15 min, maintained at a pressure range of 0.3 to 0.6 atm. Subsequent to six minutes of nitrogen bubbling, 10% of the fondant should be sprinkled on the surface of the metal bath. During the process of degassing with nitrogen, the temperature of the liquid alloy increased to 740 °C. Subsequent to the completion of degassing, the bath was maintained in a state of quiescence for a duration of six minutes. Subsequent to this operation, alloying with the pre-alloys of Al-Mg and Al-Ti was performed.

The alloy obtained was subsequently discharged into the casting pot, where degassing was continued with the other quantity of almed pellets. Subsequently, the metal bath was left undisturbed for a period of five minutes. Following this interval, the slag was meticulously cleaned, and 20% of the fondant quantity was dispersed. The alloy bath was modified through the gradual introduction of fondant capsules into the bell, which was equipped with perforations, at a temperature of 740 °C.

These capsules were stored at the base of the metal bath, commonly referred to as the "pot," until the moment when a reddish flame emerged on the surface of the metal bath. Subsequent to this initial stage, the bell was subjected to a process of agitation within the liquid metal bath, a process that continued until the entirety of the fondant was utilized. Thereafter, the alloy was permitted to undergo a period of settling for a duration of ten minutes. At the conclusion of the modification process, a sample was collected, and if it exhibited a blue coloration within the initial seconds, it can be deduced that the modification was executed successfully. At an elevated temperature of 710 °C, the process of cleaning the slag was initiated. Concurrently, at a temperature of 700 °C, the centrifugal casting of the matrix material into the fiberglass preform commenced. The chemical composition of the aluminum matrix determined by means of UV-spectroscopy (Spectromaxx, Spectro Ametek, Kleve, Germany) can be found in Table 1.

2.3. Preparation of Insert Material and the Samples

The mesh/fiber insert underwent a thorough mechanical cleaning process to remove impurities. This was followed by a degreasing procedure in trichloroethylene, a highly effective cleaning agent, and a drying step in a hot air stream. The steel mesh facilitated the infiltration of the molten metal and improved the bonding between the interfaces [38–41].

It is anticipated that the implementation of this operation will result in a reduction of the contact angle to within the range of 60° to 76°. The chemical composition of the insert is enumerated in Table 2.

In order to enhance the wetting conditions between the matrix and the insert, as well as to achieve a composite material of higher quality, the steel mesh was coated with copper by means of galvanization.

The formation of intermetallic compounds by copper has been demonstrated to enhance interface hardness and mechanical properties. Additionally, copper has been observed to function as a diffusion barrier [42–44]. The application of the copper layer was carried out through a sequence of operations, consisting of predegreasing, degreasing and pickling, alkaline copper plating, acid copper plating with sulfate, and finally passivation of the deposited layer. Subsequent to the application of the copper layer, a preheating of the fibers was performed to achieve an optimal bond between the matrix and the steel fibers. The preheating was conducted at a temperature ranging from 600 to 620 °C.

To obtain a flat composite, the cylindrical samples were subjected to a rolling process. The rolling process was executed at low temperatures on a reversible rolling mill, which was custom-built, and exhibited the following technical specifications: roller diameter: 60 mm, plate length: 1100 mm, distance between pressure screws: 140 mm, motor power (roller track drive motor and roller drive motor): 2.5 kW, speed: 1500 rpm, and maximum width of the rolled sheet: 100 mm. Prior to the rolling process, the component underwent a mechanical cleaning procedure to eliminate impurities. The cast semi-finished product was also pickled in a sodium hydroxide (NaOH) solution.

2.4. Microstructural Investigation and Tensile Test

Microstructural investigations of the coatings were conducted on cross-sectional samples by means of scanning electron microscopy (SEM/FEI Company, Philips XL 30 ESEM, Eindhoven, The Netherlands) combined with energy dispersive X-ray analysis (EDX from EDAX, Wiesbaden, Germany).

A Mecmesin Multitest 2.5 dV machine (PPT Group UK Ltd., Slinfold, UK) was used to carry out the tensile tests (according to SR EN ISO/CEI 17025:2005 [45]). A total of eight specimens (50 mm × 10 mm × 2 mm, cut by universal sheet metal guillotine) were subjected to testing to assess the reproducibility of the ultimate tensile strength (UTS). The primary objective was to ascertain the consistency of the results across multiple samples without the necessity of conducting statistical calculations.

3. Experimental Results

3.1. Microstructural Characterization

The fractured surface of the composite material (see Figure 2) revealed the Al-base matrix material, the reinforcement (mesh/fiber insert), and the copper intermediary layer. The latter was applied on the insert to improve the adhesion to the matrix and, moreover, to improve the mechanical characteristics. The presence of a uniform and well-distributed copper layer on the insert surface is known to result in optimal adhesion along the interface. This, in turn, has been shown to reduce the risk of brittle Al-Fe phase formation.

EDX spectroscopy provides information on the elemental composition of the composite material. As illustrated in Figure 3, the analysis of the spectrum indicates that aluminum is the primary element in the matrix structure, accompanied by other components that enhance the durability and mechanical strength of the composite (e.g., Cu, Zn, Mg, Si). The detected oxygen is likely derived from residual oxides (Al_2O_3, MgO, TiO_2), which are formed during the processing of waste and the melting of pre-alloys in the elaboration process.

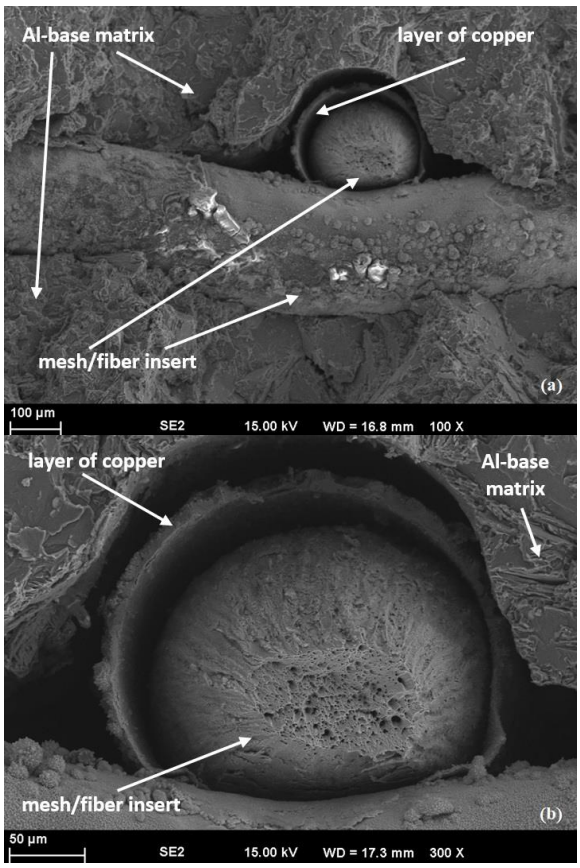


Figure 2. SEM-micrographs of the fractured surface of the composite material: (**a**) magnification 100×; (**b**) 300× magnification.

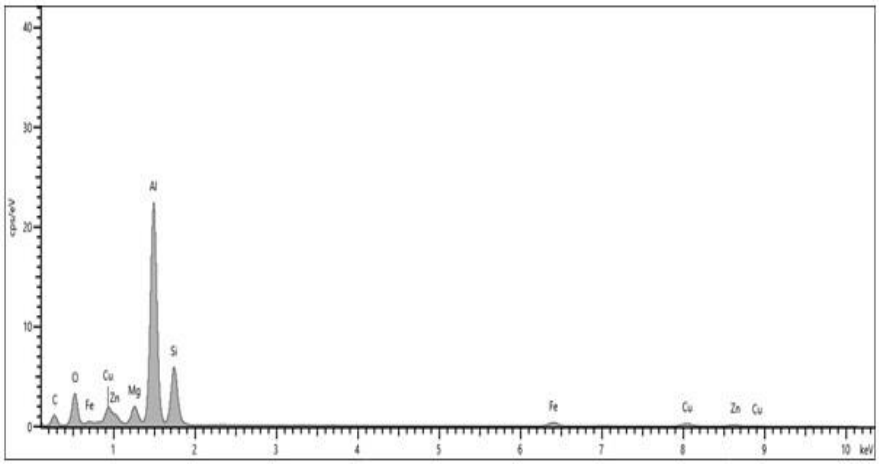


Figure 3. EDX analysis of composite material.

3.2. Tensile Test

The tensile strength of the specimens (eight samples) was determined by applying a constant force until the specimen broke relative to its cross-sectional area [46]. The results of this study are presented in Table 3.

$$\sigma = \frac{F_{max}}{a \cdot b[N/\mathrm{mm}^2]} \quad (1)$$

where F_{max} is the loading force, unit stress [N]; a, b—specimen section [mm^2].

Table 3. Physical parameters required for calculating tensile strength.

Sample/Parameters	a [mm]	b [mm]	F max [N]	σ [N/mm^2] $\times$ 10^3
T1	15.7	15.1	28.40	119.80
T2	15.4	15.0	24.89	107.75
T3	15.5	15.0	23.01	98.97
T4	15.6	15.1	18.50	78.54
T5	15.3	15.0	26.69	116.30
T6	15.2	15.1	24.00	104.57
T7	15.6	15.0	23.50	100.43
T8	15.4	15.1	22.92	98.56

A thorough examination of the fractured surfaces following the tensile testing of the samples, which demonstrated extreme values for breaking strength, reveals that the low value of sample 4 (T4) was predominantly attributable to failure (pull-out) along the interface with the matrix. As illustrated in Figure 4, the microstructure surrounding the insert may exhibit characteristics that differ from the overall surface structure, potentially presenting a finer grain or harder areas. This phenomenon was further substantiated by the graphical representation of the data processing, which manifested as a bimodal distribution (see Figure 5). It is conceivable that during the casting process, the effect of centrifugal force may influence the distribution of the intermetallic phases. It is noteworthy that in all the samples examined, the fracture occurred without any evidence of deformation, with the break surface being perpendicular to the direction of stress. This observation indicates a brittle break behavior.

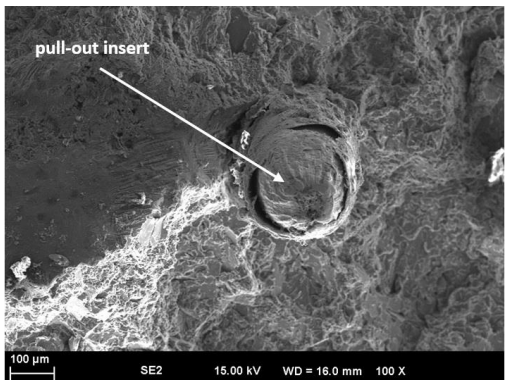


Figure 4. SEM-micrograph of the fractured surface after tensile testing of sample T4.

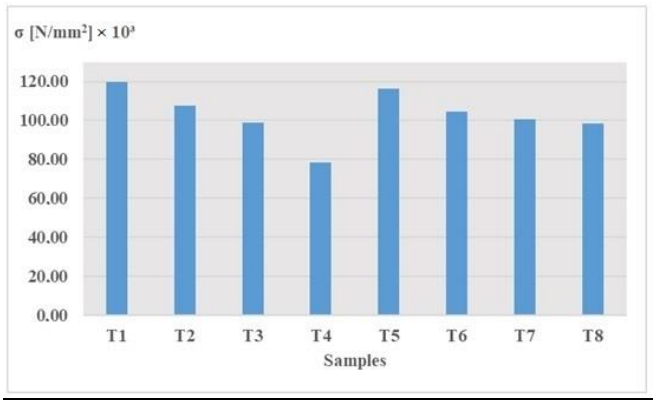


Figure 5. Bimodal distribution of breaking load force values.

Another potential cause of inappropriate behavior may be the distribution of steel mesh in the composite matrix. In the event that the mesh positioning is not identical in all samples, this can result in the presence of locally weaker or stronger areas in the composite, which is reflected in the breaking strength. As illustrated in Figure 6, the analytical curve is presented through the use of polynomial interpolation. This suggests a reasonable correlation between the mathematical model and the real data. At the same time, it recorded the following relationship of the mean squared deviation ($R^2 = 0.6388$): $y = 0.2184x^5 - 4.9466x^4 + 40.691x^3 - 145.99x^2 + 212.05x + 17.298$.

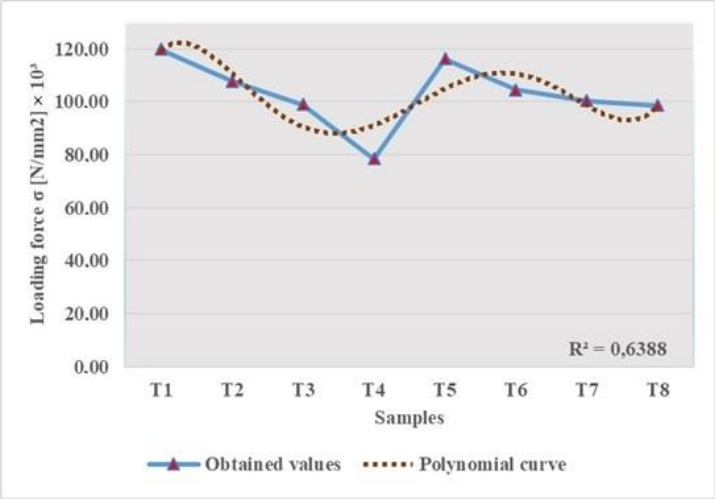


Figure 6. Distribution of load forces at break and analytical curve.

4. Results and Discussion

In addition to the increased tensile strength observed for the steel mesh-reinforced aluminum matrix composite, the results indicate improved structural integrity and load-bearing capacity. The higher tensile values suggest efficient stress transfer across the matrix–reinforcement interface, which is attributable to the surface preparation (copper coating and preheating) of the steel mesh. A thorough microstructural examination was conducted, yielding findings that substantiate the uniform distribution of the matrix within the steel mesh wires. This distribution was characterized by the absence of substantial porosity or detachment zones, suggesting a well-defined and consistent arrangement of the matrix around the wires. This uniform adhesion contributed to the mechanical performance of the material, acting as an effective barrier to crack propagation under tensile load. Fracture surface observations provide further evidence to support these findings. The reinforced samples demonstrated a combination of fracture modes, exhibiting evidence of ductile tearing within the aluminum matrix and crack deflection in proximity to the mesh interface. The presence of these features is indicative of enhanced energy absorption and local toughening mechanisms. The performance of the composite was found to be strongly influenced by the interface quality between the steel mesh and the aluminum matrix. The efficacy of adhesion was maximized through the implementation of copper plating and thermal pre-treatment of the insert, thereby facilitating efficient load transfer and mitigating stress concentration zones. The observation of an absence of interfacial voids or delamination in the microstructure lent further support to this hypothesis.

Furthermore, the fracture mode observed suggests that the steel mesh acted as a mechanical barrier, diverting crack propagation and contributing to energy dissipation during fracture. This mechanism elucidated the enhanced tensile strength observed and posits prospective advantages for applications necessitating augmented structural integrity under mechanical stress.

5. Conclusions

The process of casting the aluminum alloy directly onto a steel mesh insert presented a series of challenges, particularly with regard to the interface between the two materials. Ensuring adequate wetting and adhesion at the interface was identified as a primary concern, given its critical role in establishing a robust and durable bond between the aluminum matrix and the steel mesh. Insufficient wetting could result in weak points or incomplete bonding, which would jeopardize the structural integrity of the composite. In order to mitigate this issue, a copper intermediary layer was applied to the steel insert prior to casting. This copper layer was found to be highly effective in improving the metallurgical compatibility between the steel and aluminum. The material under consideration functioned as a bonding interface, thereby enhancing adhesion and minimizing the risk of defects at the interface. Consequently, it ensured a more dependable and cohesive bond between the matrix material and the steel mesh.

The experimental results from tensile testing demonstrated that the failure forces across various specimens exhibited a relatively narrow range of variation. Specifically, the tensile failure forces exhibited a range of approximately 78.54–119.80 N. This limited dispersion suggests a certain degree of consistency in the manufacturing process, although residual variability persisted. The observed discrepancies can be predominantly ascribed to factors inherent in the fabrication process itself, such as the precise positioning of the steel insert within the aluminum matrix during casting. The location of the insert was demonstrated to influence the material's local solidification process, thereby affecting its subsequent mechanical properties and failure behavior. It was demonstrated that variations in the position of the insert can result in differences in the microstructure and bonding quality around the interface. These variations were shown to affect the tensile strength.

Furthermore, an analytical regression curve was employed to analyze the experimental data, thereby enhancing the comprehension of the overall trend in the distribution of breaking forces. This regression model successfully encapsulates the general behavior noted in the tests and emphasizes the impact of process variability on the resulting mechanical properties. The analysis indicates that variations in the technological process—such as minor discrepancies in casting conditions, insert positioning, or cooling rates—can considerably influence the tensile strength values. In summary, the results obtained demonstrate the necessity of exercising meticulous control over manufacturing parameters to ensure the attainment of consistent and optimal bonding performance in aluminum–steel composites.

Author Contributions: Conceptualization, R.B.-N. and C.R.C.; methodology, R.B.-N., C.-O.M. and C.R.C.; validation, R.B.-N., C.-O.M., C.R.C. and G.M.; formal analysis, C.-O.M. and C.R.C.; investigation, G.M., C.R.C., C.-O.M. and R.B.-N.; resources, R.B.-N., C.R.C. and C.-O.M.; writing—original draft preparation, C.R.C. and G.M.; writing—review and editing, C.R.C., C.-O.M. and G.M.; visualization, C.R.C. and C.-O.M.; supervision, G.M. and R.B.-N. All authors have read and agreed to the published version of the manuscript.

Funding: The publication of this article was supported by the 2024 Development Fund of the UBB.

Data Availability Statement: The original contributions presented in the study are included in the article, and further inquiries can be directed to the corresponding author.

Conflicts of Interest: The authors declare no conflicts of interest.

References

1. Samal, P.; Vundavilli, P.; Meher, A.; Mahapatra, M. Recent progress in aluminum metal matrix composites: A review on processing, mechanical and wear properties. *J. Manuf. Process.* **2020**, *59*, 131–152. [CrossRef]
2. Imran, M.; Khan, A. Characterization of Al-7075 metal matrix composites: A review. *J. Mater. Res. Technol.* **2019**, *8*, 3347–3356. [CrossRef]

3. Ashebir, D.; Mengesha, G.; Sinha, D. An Insight into Mechanical and Metallurgical Behavior of Hybrid Reinforced Aluminum Metal Matrix Composite. *Adv. Mater. Sci. Eng.* **2022**, *2022*, 7843981. [CrossRef]
4. Koli, D.; Agnihotri, G.; Purohit, R. Advanced Aluminium Matrix Composites: The Critical Need of Automotive and Aerospace Engineering Fields. *Mater. Today Proc.* **2015**, *2*, 3032–3041. [CrossRef]
5. Prasad, S.; Asthana, R. Aluminum Metal-Matrix Composites for Automotive Applications: Tribological Considerations. *Tribol. Lett.* **2004**, *17*, 445–453. [CrossRef]
6. Suthar, J.; Patel, K. Processing issues, machining, and applications of aluminum metal matrix composites. *Mater. Manuf. Process.* **2018**, *33*, 499–527. [CrossRef]
7. Kumar, A.; Singh, V.; Singh, R.; Chaudhary, R.; Kumar, D.; Mourad, A. A review of aluminum metal matrix composites: Fabrication route, reinforcements, microstructural, mechanical, and corrosion properties. *J. Mater. Sci.* **2024**, *59*, 2644–2711. [CrossRef]
8. Che, J.; Kim, J.; Lee, H.; Chang, S. Application of carbon/epoxy composites to robot console structure for high stiffness with lightweight. *Compos. Struct.* **2022**, *300*, 116121. [CrossRef]
9. Chak, V.; Chattopadhyay, H.; Dora, T. A review on fabrication methods, reinforcements and mechanical properties of aluminum matrix composites. *J. Manuf. Process.* **2020**, *56*, 1059–1074. [CrossRef]
10. Tenali, N.; Ganesan, G.; Ravindra Babu, P. An Investigation on the Mechanical and Tribological Properties of an Ultrasonic-Assisted Stir Casting Al-Cu-Mg Matrix-Based Composite Reinforced with Agro Waste Ash Particles. *Appl. Eng. Lett.* **2024**, *9*, 46–63. [CrossRef]
11. Krstić, J.; Jovanović, J.; Gajević, S.; Miladinović, S.; Vaxevanidis, N.; Kiss, I.; Stojanović, B. Application of Metal Matrix Nanocomposites in Engineering. *Adv. Eng. Lett.* **2024**, *3*, 180–190. [CrossRef]
12. Moghadam, A.D.; Schultz, B.F.; Ferguson, J.; Omrani, E.; Rohatgi, P.K.; Gupta, N. Functional Metal Matrix Composites: SelfLubricating, Self-Healing, and Nanocomposites-An Outlook. *JOM* **2014**, *66*, 872–881. [CrossRef]
13. Chelladurai, S.; Kumar, S.; Venugopal, N.; Ray, A.; Manjunath, T.; Gnanasekaran, S. A review on mechanical properties and wear behaviour of aluminium based metal matrix composites. *Mater. Today Proc.* **2020**, *37 Pt 2*, 908–916S. [CrossRef]
14. Sowrabh, B.S.; Gurumurthy, B.M.; Shivaprakash, Y.M.; Sharma, S. Reinforcements, production techniques and property analysis of AA7075 matrix composites—A critical review. *Manuf. Rev.* **2021**, *8*, 31. [CrossRef]
15. Maleque, M.; Adebisi, A. Energy efficient lighter weight aluminium matrix composite automotive brake motor. In Proceedings of the International Conference Harnessing Technology 2011, Singapore, 14–16 July 2011.
16. Gomilšek, R.; Čuček, L.; Homšak, M.; Tan, R.; Kravanja, Z. Carbon Emissions Constrained Energy Planning for Aluminum Products. *Energies* **2020**, *13*, 2753. [CrossRef]
17. Bhoi, N.; Singh, H.; Pratap, S. Developments in the aluminum metal matrix composites reinforced by micro/nano particles—A review. *J. Compos. Mater.* **2020**, *54*, 813–833. [CrossRef]
18. Vellaichamy, R.D.; Tharisanan, R.; Allahpitchai, M.; Krishnan, B. Investigate the mechanical properties of Aluminium Metal Matrix Composite. *J. Phys. Conf. Ser.* **2024**, *2748*, 012009. [CrossRef]
19. Saravanan, G.; Bhaskar, G.; Elaiyarasan, U.; Alagu, R. A study on mechanical and microstructure behaviour of carbon and glass fibre reinforced Al 2024-T3 laminated composite. *Metall. Res. Technol.* **2023**, *120*, 203. [CrossRef]
20. Ramdani, N.; Razali, M. Processing, Properties, and Uses of Lightweight Glass Fiber/Aluminum Hybrid Structures. In *Handbook of Research on Advancements in the Processing, Characterization and Application of Lightweight Materials*; IGI Global Scientific Publishing: Hershey, PA, USA, 2022; ISBN 9781799878643. [CrossRef]
21. Khalid, M.; Arif, Z.; Rashid, A.; Shahid, M.; Ahmed, W.; Tariq, A.; Abbas, Z. Interlaminar shear strength (ILSS) characterization of fiber metal laminates (FMLs) manufactured through VARTM process. *Forces Mech.* **2021**, *4*, 100038. [CrossRef]
22. Samal, P.; Raj, H.; Meher, A.; Surekha, B.; Vundavilli, P.; Sharma, P. Synergistic Effect of B4C and Multi-Walled CNT on Enhancing the Tribological Performance of Aluminum A383 Hybrid Composites. *Lubricants* **2024**, *12*, 213. [CrossRef]
23. Thiraviam, R.; Ravisankar, V.; Pradeep Kumar, K.; Thanigaivelan, R.; Arunachalam, R. A novel approach for the production and characterisation of aluminium–alumina hybrid metal matrix composites. *Mater. Res. Express* **2020**, *7*, 046512. [CrossRef]
24. Ponnusamy, P.; Rashid, R.A.R.; Masood, S.H.; Ruan, D.; Palanisamy, S. Mechanical Properties of SLM-Printed Aluminium Alloys: A Review. *Materials* **2020**, *13*, 4301. [CrossRef] [PubMed]
25. James, J.; Annamalai, A.; Muthuchamy, A.; Jen, C. Effect of Wettability and Uniform Distribution of Reinforcement Particle on Mechanical Property (Tensile) in Aluminum Metal Matrix Composite A Review. *Nanomaterials* **2021**, *11*, 2230. [CrossRef] [PubMed]
26. Kalashnikov, I.; Kobeleva, L.; Bykov, P.; Kolmakov, A.; Katin, I.; Mikheev, R. Estimation of distribution uniformity of Ti2NbAl particles in an aluminum-matrix composite material. *Perspekt. Mater.* **2022**, *5*, 40–48. [CrossRef]
27. Malaki, M.; Tehrani, F.; Niroumand, B.; Gupta, M. Wettability in Metal Matrix Composites. *Metals* **2021**, *11*, 1034. [CrossRef]
28. Yang, X.; Barekar, N.; Ji, S.; Dhindaw, B.; Fan, Z. Influence of reinforcing particle distribution on the casting characteristics of Al-SiCp composites. *J. Mater. Process. Technol.* **2020**, *279*, 116580. [CrossRef]

29. Wang, Y.; Zhang, J. A Review of the Friction and Wear Behavior of Particle-Reinforced Aluminum Matrix Composites. *Lubricants* **2023**, *11*, 317. [CrossRef]
30. Zhang, X.; Hu, T.; Rufner, J.; Lagrange, T.; Campbell, G.; Lavernia, E.; Schoenung, J.; Van Benthem, K. Metal/ceramic Interface Structures and Segregation Behavior in Aluminum-based Composites. *Microsc. Microanal.* **2015**, *21*, 1053–1054. [CrossRef]
31. Gowrishankar, M.C.; Hiremath, P.; Shettar, M.; Sharma, S.; SatishRao, U. Experimental validity on the casting characteristics of stir cast aluminium composites. *J. Mater. Res. Technol.* **2020**, *9*, 3340–3347. [CrossRef]
32. Zhu, J.; Jiang, W.; Li, G.; Guan, F.; Yu, Y.; Fan, Z. Microstructure and mechanical properties of SiCnp/Al6082 aluminum matrix composites prepared by squeeze casting combined with stir casting. *J. Mater. Process. Technol.* **2020**, *283*, 116699. [CrossRef]
33. Lee, Y.; Kim, N.; Lee, S.; Kim, Y.; Cho, S.; Lee, S.; Jo, I. Microstructure and mechanical properties of lightweight TiC-steel composite prepared by liquid pressing infiltration process. *Mater. Charact.* **2020**, *162*, 110202. [CrossRef]
34. Rathee, S.; Maheshwari, S.; Siddiquee, A. Issues and strategies in composite fabrication via friction stir processing: A review. *Mater. Manuf. Process.* **2018**, *33*, 239–261. [CrossRef]
35. Sharma, A.; Sharma, V.; Mewar, S.; Pal, S.; Paul, J. Friction stir processing of Al6061-SiC-graphite hybrid surface composites. *Mater. Manuf. Process.* **2018**, *33*, 795–804. [CrossRef]
36. *SR EN 1676:2020*; Aluminium and Aluminium Alloys. Ingots for Remelting of Aluminum Alloys. Specifications. European Committee for Standardization (CEN): Brussels, Belgium, 2020.
37. Belu-Nica, R. *Contributions on the Production and Joining by Welding of Thin Sheets Made of Metal Composite Materials with Aluminum Alloy Matrix*; Politehnica Publishing House: Timişoara, Romania, 2007; Volume 9.
38. Szczepanik, S. Composites of Aluminium Alloy Matrix Reinforced by a Steel Mesh. *Mater. Today Proc.* **2015**, *2*, S9–S18. [CrossRef]
39. Ferro, P.; Fabrizi, A.; Bonollo, F.; Berto, F. Microstructural and mechanical characterization of a stainless-steel wire mesh–reinforced Al-matrix composite: Bimatallic components for lightweight design. *Frat. Ed Integr. Strutt.* **2020**, *15*, 289–301. [CrossRef]
40. Chelladurai, S.; Arthanari, R.; Krishnamoorthy, K.; Selvaraj, K.; Govindan, P. Effect of Copper Coating and Reinforcement Orientation on Mechanical Properties of LM6 Aluminium Alloy Composites Reinforced with Steel Mesh by Squeeze Casting. *Trans. Indian Inst. Met.* **2018**, *71*, 1041–1048. [CrossRef]
41. Huang, H.; Wang, J.; Liu, W. Mechanical properties and reinforced mechanism of the stainless steel wire mesh–reinforced Al-matrix composite plate fabricated by twin-roll casting. *Adv. Mech. Eng.* **2017**, 1–9. [CrossRef]
42. Weng, H.; Wang, J.; Zhu, X.; Lu, X. Effect of heat treatment on interfacial microstructure and mechanical properties of the aluminum/steel joints with copper transition layer. *Intermetallics* **2025**, *178*, 108646. [CrossRef]
43. Wang, G.; Zhou, K.; Ren, B.; Yu, W. Influence of Cu/Ni coating on microstructure and mechanical properties in steel/aluminum single-sided resistance spot welding joint. *J. Mater. Process. Technol.* **2025**, *335*, 118675. [CrossRef]
44. Khoonsari, E.; Jalilian, F.; Paray, F.; Emadi, D.; Drew, R. Interaction of 308 stainless steel insert with A319 aluminium casting alloy. *Mater. Sci. Technol.* **2010**, *26*, 833–841. [CrossRef]
45. *SR EN ISO/CEI 17025:2005*; General Requirements for the Competence of Testing and Calibration Laboratories. European Committee for Standardization (CEN): Brussels, Belgium, 2005.
46. Mănescu, T. *Applications of Material Strength*; Eftimie Murgu: Reșița, Romania, 2010.

Disclaimer/Publisher's Note: The statements, opinions and data contained in all publications are solely those of the individual author(s) and contributor(s) and not of MDPI and/or the editor(s). MDPI and/or the editor(s) disclaim responsibility for any injury to people or property resulting from any ideas, methods, instructions or products referred to in the content.